Supporting information for "Guided Assembly of Metal and Hybrid Conductive Probes Using Floating Potential Dielectrophoresis"

Josep Puigmartí-Luis,[a] Johannes Stadler,[a] Daniel Schaffhauser,[a] Ángel Pérez del Pino,[b] Brian R. Burg[c] and Petra S. Dittrich*[a]*

[a] Department of Chemistry and Applied Biosciences, ETH Zürich, 8093 Zürich, Switzerland.
[b] Institut de Ciéncia de Materials de Barcelona (CSIC), Campus Universitari, 08193 Bellaterra, Spain.
[c] Department of Mechanical and Process Engineering, ETH Zürich, 8092 Zürich, Switzerland.
Corresponding author email address: puigmarti.luis@org.chem.ethz.ch; dittrich@org.chem.ethz.ch

Additional AFM, SEM and EDX analysis of the micro- and nanowires, as well as cyclic voltammetry (CV) studies of the solutions

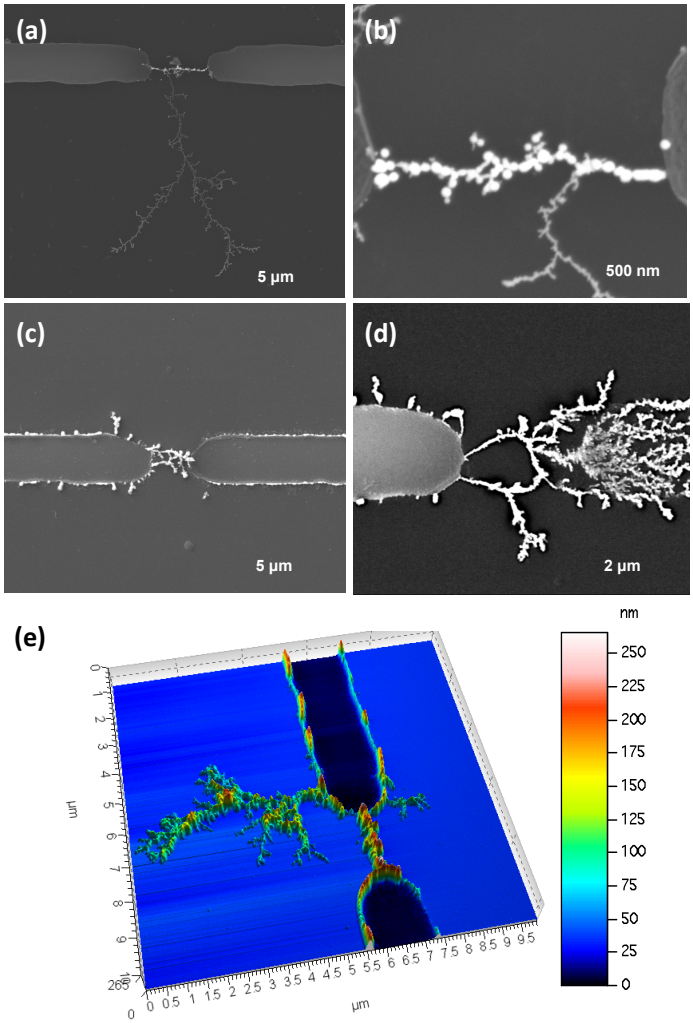

Figure S1. SEM images of (a) and (b) TTF-Au nanowires and (c) and (d) bare gold nanowires bridging electrode pairs. Growth of nanowires occurs preferentially at the electrode edges (location

of highest field gradient), and the formation of branches is observed. (e) Topographic AFM image of a hybrid TTF-Au wire grown between electrodes 2 μm apart.

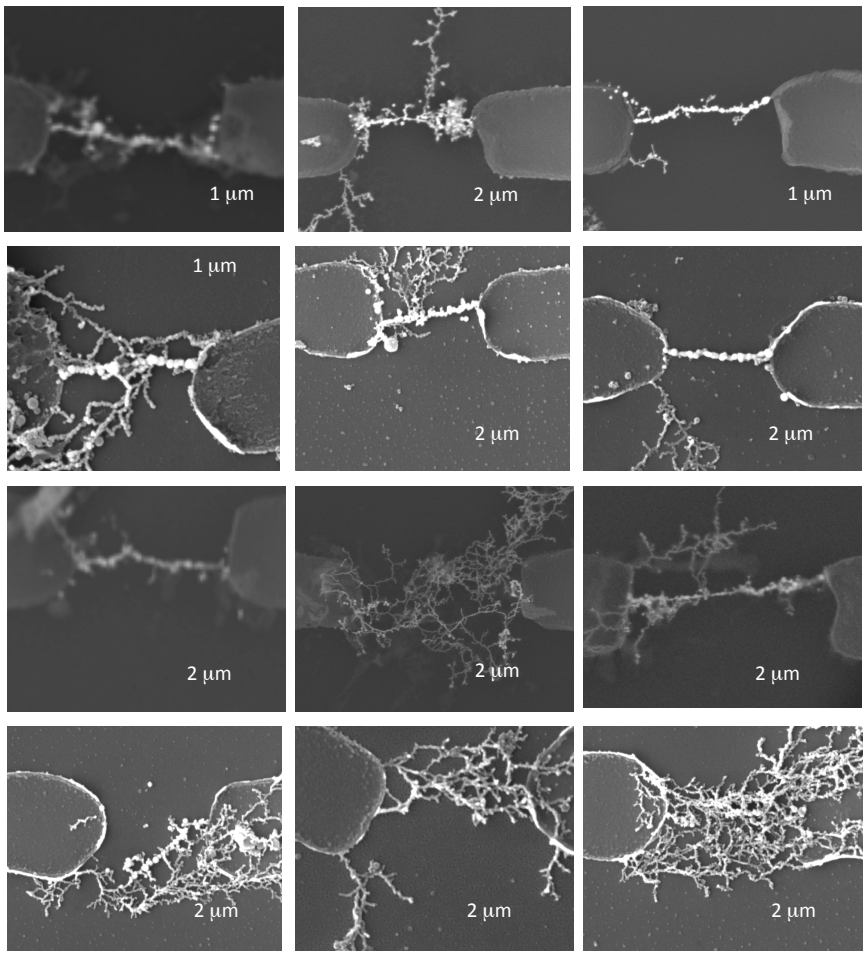

Figure S2. Representative collection of SEM images of different TTF-Au microjuntions produced by floating potential dielectrophoresis.

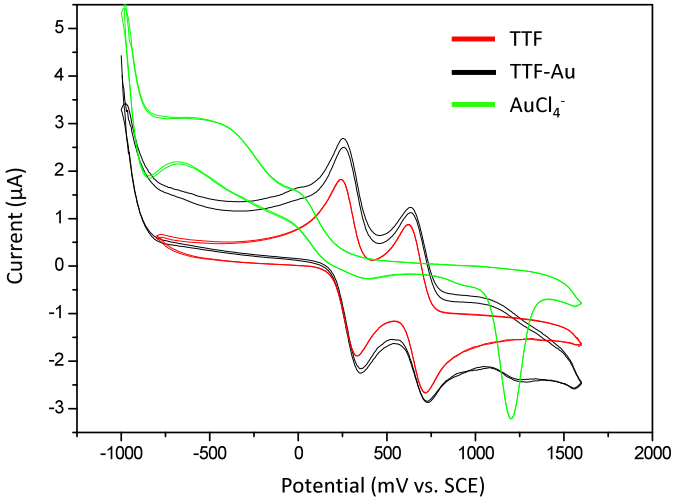

Figure S3. Cyclic voltammograms measured in acetonitrile (0.1 M Bu_4NPF_6) of; TTF (red), TTF-Au (black) and hydrogen tetrachloroaurate (green). The measurements were performed at room temperature and the scan rate was 100 mV s^{-1}.

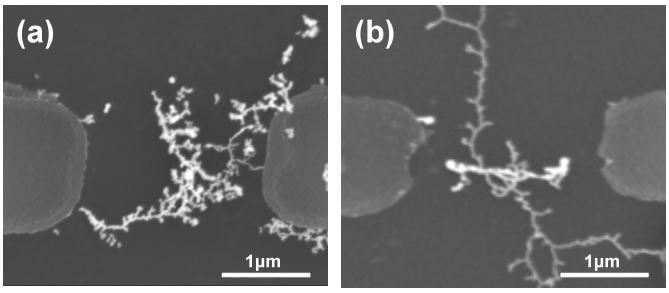

Figure S4. SEM images of TTF-Au wires after applying voltages above 1V. The images show how the contacts of the wires and the electrodes broke down.

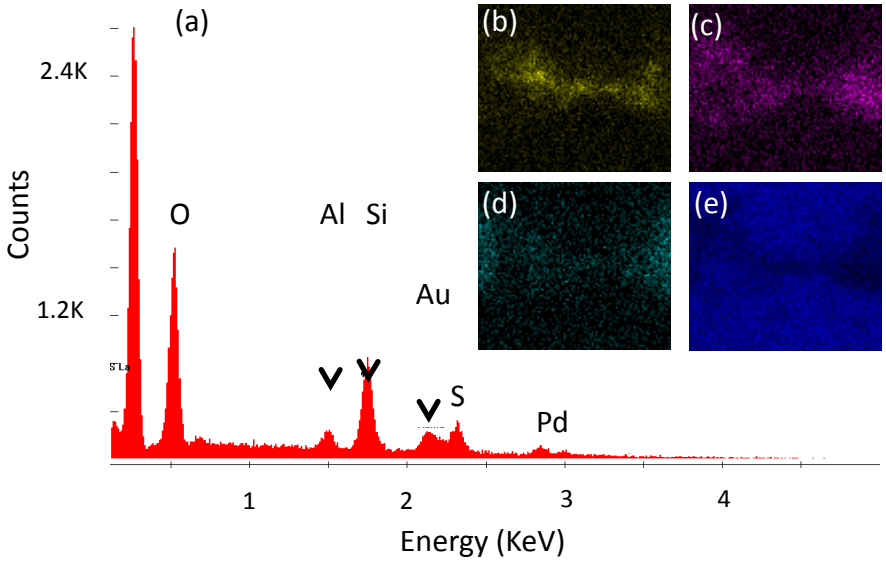

Figure S5. (a) Individual EDX spectra of a TTF-Au hybrid wire assembled using floating potential dielectrophoresis. EDX maps for (b) gold, (c) sulphur, (d) palladium and (e) oxygen. The spectra and the EDX maps clearly show that the hybrid wires are made up of S, from the TTF molecules, and gold. Furthermore, the hybrid wires have a uniform S and Au distribution between the palladium electrode pair as indicated by the element maps.

SERS measurements on a bare gold wire

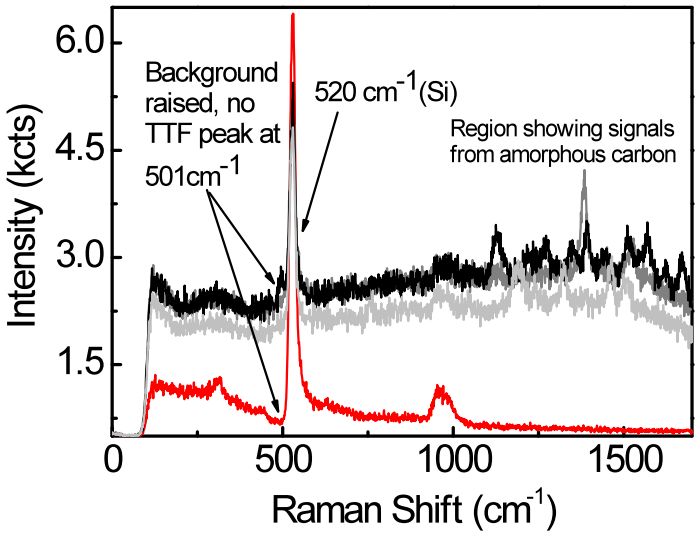

Figure S6. All spectra are from a chip where pure gold wires were synthesized without TTF (10 s, 632.8 nm, 100 μW power). The red spectrum shows background signals from the pure Si chip – all bands can be attributed to Si. The black and grey spectra are taken from 3 points within the gold wire area exhibiting a raised overall background without visible TTF bands. Weak bands from amorphous

carbon are visible in the region of 1000-1600 cm^{-1}. This area can potentially enhance Raman signals, but no clear signatures are present due to the lack of analytes.

Experimental Section

Synthesis of tetrathiafulvalene-gold (TTF-Au) cation-radical solution and characterisation:

In a typical experiment, 50 µl of hydrogen tetrachloroaurate solution (Aldrich, 0.006 mM) was added to a solution of TTF (Acros, 0.8 mM), both in acetonitrile. The reaction mixture was left overnight, the precipitate was removed, and the filtrate was collected. The resulting brownish solution was the sample used for the dielectrophoretic assembly of TTF-Au wires.

The presence of TTF cation-radical ($TTF^{+\bullet}$) and gold ions in the precursor solution was confirmed by Electron Paramagnetic Resonance (EPR) spectroscopy and X-ray Photoelectron Spectroscopy (XPS) measurements, respectively. In the EPR analysis, a characteristic peak of an organic free radical with a g-value of 2.004 was determined[1] (Figure S5a) and TTF cation-radical bands located at 437 nm and 579 nm were also found by UV-vis spectroscopy which provides the most conclusive evidence of cation-radicals of TTF in solution (Figure S5b).[2,3]

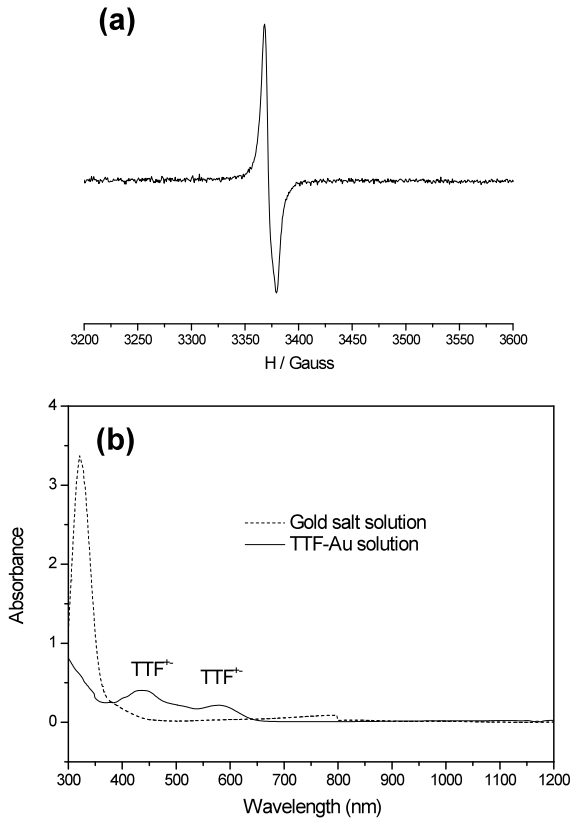

Figure S7. (a) EPR spectrum of the TTF-Au solution measured at 77 K. (b) UV-vis spectra of TTF-Au solution showing the TTF cation radical band located at 579 nm (i), and (ii) UV-vis spectra of a gold salt solution.

On the other hand, XPS spectroscopy studies confirmed the presence of gold ions in the TTF-Au solution. A binding energy located above 84.0 eV in the XPS spectra of TTF-Au sample suggests the presence of Au^{+} species (Figure S6b).[4] For comparison, an XPS spectrum of gold in its purely metallic state is also presented (Figure S6a).

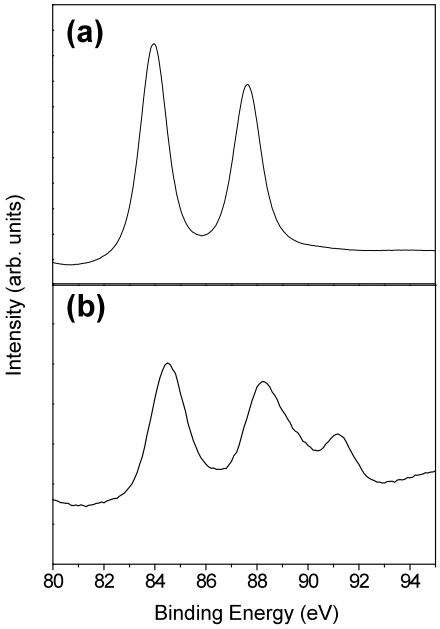

Figure S8. XPS spectra of (a) gold in its purely metallic state (reference) and (b) TTF-Au solution.

Further characterisation of the TTF-Au sample by means of Transmission Electron Microscopy (TEM) analysis confirmed the absence of nanoparticles in solution. The images show some organic residues, which were manly composed of S and Cl ions as demonstrated by Energy-dispersive X-ray spectra (EDX) (Figure S7).

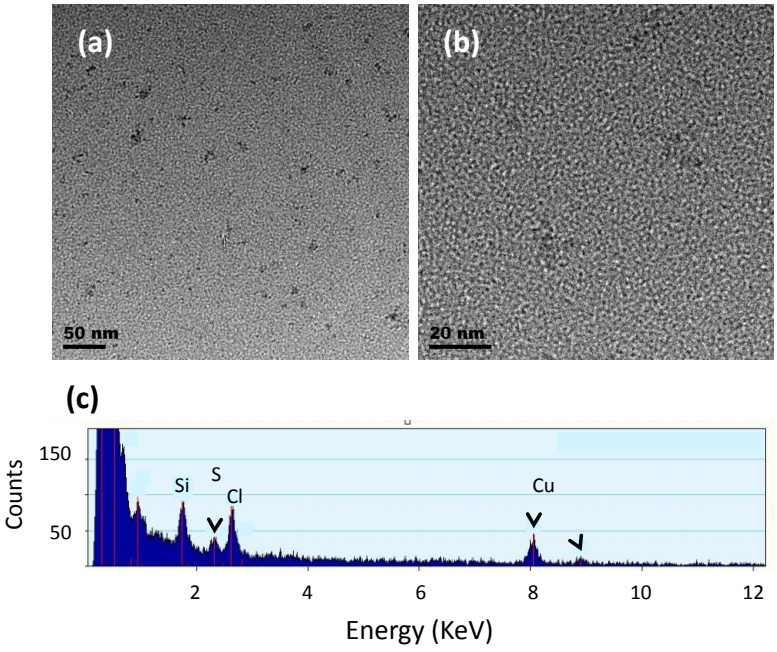

Figure S9. (a) and (b) are TEM images of the TTF-Au sample after evaporation on a holey-carbon TEM grid. (c) EDX spectra of the aggregates.

Chip fabrication and electronic characterisation:

A detailed description of the chip and the fabrication protocols are given in references 5 and 6. Briefly, a p-doped silicon substrate was covered with an insulating dry thermal gate oxide layer

(t_{ox}=285 nm). The 50 nm-thick Pd electrodes with a gap of 2 μm were fabricated using standard lithography and lift-off techniques. The final chip had a size of 2 mm x 4 mm and contained 20 individually electrode gaps. For operation, the bias electrode and the p-doped silicon substrate are connected to an arbitrary function generator (LeCroy LW420B). After placing a drop of precursor solution onto the chip surface, a sinusoidal potential difference to the contacted electrodes was applied (5 V_p at a frequency of 1 MHz).

The electrical characterisation was carried out using a probe station connected to a Keithley 4200 *I-V* characterisation system under ambient conditions.

AFM and confocal Raman measurements:

AFM and confocal Raman measurements were conducted on a confocal Raman system (Spectra upright, NTMDT, Russia) using a 100x100x10 μm piezo scanner, contact mode cantilevers (ATEC-CONT, NanoSensors, Switzerland), a 100x 0.7 NA objective (Mitutoyo, Japan) and a 632.8 nm HeNe laser.

Surface-enhanced Raman spectroscopy (SERS) spectra were obtained on an inverted optical microscope (IX70, Olympus, Japan) using a 532 nm DPSS laser (Ventus, Laser Quantum, UK) and a 60x1.4 NA oil immersion objective. SERS substrates were vapor coated by resistive heating (EM Med 020, Leica, Germany) with 6 nm of Ag (Aldrich, 99.99%) at $5x10^{-6}$ mbar, after cleaning in piranha acid solution for 1h and subsequent rinsing with MeOH. AFM topography measurements working in intermittent contact mode were carried out with an Agilent 5500LS system.

Current-sensing AFM (CS AFM):

All measurements were carried out under normal atmospheric conditions with an Agilent 5500LS apparatus equipped with a Resiscope module. In these studies, the common electrode pad was wire-bonded to a metallic support (Fig. 3a). A contact to the metal support using a stainless steel clamp enabled application of a bias voltage to the large electrode pad on the chip while scanning with a grounded conductive Pt-Ir coated silicon tip. Consequently, the CS-AFM images show the current flow through the conductive parts on the chip.

SEM and TEM measurements:

The SEM images were obtained using a FEI Quanta 200 FEG. TEM and the energy dispersive X-ray spectroscopy were measured with a Philips CM 12 operating at 120 kV.

XPS and UV-vis characterisation:

X-Ray photoelectron spectroscopy measurements were conducted on a Sigma2 XPS (Thermo Fischer Scientific Inc., Loughborough, GB). The source was non-monochromated Mg (200 W). The analysis was conducted on a large area with a diameter of 500 μm. The UV–vis spectra were recorded using a Cary 5000 UV–vis–near-IR spectrophotometer.

References (for Supporting information):

1 L. R. C. Barclay and M. R. Vinqvist, *Free Radic. Biol. Med.*, 1994, **16**, 779.

2 K. Naka, D. Ando, X. Wang and Y. Chujo, *Langmuir*, 2007, **23**, 3450.

3 J. Puigmartí-Luis, D. Schaffhauser, B. R. Burg and P. S. Dittrich, *Adv. Mat.*, 2010, **22**, 2255.

4 a) Z. Huo, Ch.-K. Tsung, W. Huang, X. Zhang and P. Yang, *Nano Lett.*, 2008, **8**, 2041; b) Ch. Zhou, C. Sun, M. Yu, Y. Qin, J. Wang, M. Kim, and J. Zheng, *Langmuir*, 2010, **114**, 7727.

5 B. R. Burg, J. Schneider, M. Muoth, L. Durrer, T. Helbling, N. C. Schirmer, T. Schwamb, Ch. Hierold and D. Poulikakos, *Langmuir*, 2009, **25**, 7778.

6 B. R. Burg, V. Bianco, J. Schneider and D. Poulikakos, *J. Appl. Phys.*, 2010, **107**, 124308.